5-1-2016

Creating A Dynamic, Multi-Purpose Correction for Multiple Geometries and Field Sizes to Account for Off-Axis and Asymmetric Backscatter With Varian Portal Dosimetry

Remy Manigold
University of Nevada, Las Vegas

CREATING A DYNAMIC, MULTI-PURPOSE CORRECTION FOR MULTIPLE GEOMETRIES AND FIELD SIZES TO ACCOUNT FOR OFF-AXIS AND ASYMMETRIC BACKSCATTER WITH VARIAN PORTAL DOSIMETRY

By

Remy Yves Manigold

Bachelor of Science - Physics
California Polytechnic State University,
2014

A thesis submitted in partial fulfillment
of the requirements for the
Master of Science - Health Physics

Department of Health Physics and Diagnostic Sciences
School of Allied Health Sciences
Division of Health Sciences
The Graduate College

University of Nevada, Las Vegas
May 2016

UNLV | GRADUATE COLLEGE

Thesis Approval

The Graduate College
The University of Nevada, Las Vegas

April 14, 2016

This thesis prepared by

Remy Yves Manigold

entitled

Creating A Dynamic, Multi-Purpose Correction for Multiple Geometries and Field Sizes to Account for Off-Axis and Asymmetric Backscatter with Varian Portal Dosimetry

is approved in partial fulfillment of the requirements for the degree of

Master of Science - Health Physics
Department of Health Physics and Diagnostic Sciences

Yu Kuang, Ph.D.
Examination Committee Chair

Kathryn Hausbeck Korgan, Ph.D.
Graduate College Interim Dean

Steen Madsen, Ph.D.
Examination Committee Member

Gary Cerefice, Ph.D.
Examination Committee Member

Guogen Shan, Ph.D.
Graduate College Faculty Representative

Abstract

Intensity modulated radiation therapy and volumetric modulated arc therapy are increasingly common in radiation therapy due to their benefits of target conformity and normal tissue sparing. Due to the complexities of plan delivery and the precision required, the dose delivered must be accurately measured for quality assurance (QA). One of the most efficient ways to perform patient-specific QA when using clinical linear accelerators (linac) is to use an electronic portal imaging device (EPID). Amorphous silicon (aSi) Electronic Portal Imaging Devices (EPIDs) are attached to the linac and can provide real-time feedback with spatial resolution on the order of sub-millimeter pixel size making them very favorable for QA. However, the response to radiation in the EPIDs is not similar to that in water or soft tissue, so beam intensity profile corrections must be used and output factors specific to the imager must be collected. Additionally, when radiation exits the imager, it will travel through the support arm made up of high density materials; this non-uniform backscatter will cause the EPID to detect differences that are dependent on position and field size. To meet this need Varian Medical Systems (Palo Alto, CA) has created a 2-dimensional Portal Dosimetry Pre-Configuration (PDPC) package, which uses a 15 x 15 cm^2 matrix to correct for the asymmetric and off-axis response from the non-uniform backscatter; however, because this package is optimized for a 15 x 15 cm^2 field size, it may cause over or under correction of the backscattered radiation. The aim of this project is to correct the imager response as a function of field size for both off-axis variations and imaging arm backscatter variations. These corrections would be application-facing corrections, allowing them to be more robust than current corrections applied beyond EPID dosimetry calibration.

Acknowledgements

I would like to thank several people who played a large role in the completion of this project. First, I would like to thank my thesis advisor Dr. Kuang for always taking the time to help answer any and all questions I had during my graduate career and having faith in me. Second, I would like to thank Matthew Schmidt not only for all of his help at Varian, but for being a close mentor and friend with this project and life. Last, I would like to give a special thanks to my parents, Valerie and Yves, for loving and supporting me from day one. I would not be the man I am today without them.

Table of Contents

List of Tables

List of Figures

1) Introduction

Clinical linear accelerators (linacs) have been using more intensity modulated radiation treatment (IMRT) and volumetric arc therapy (VMAT, referred to as RapidArc when performed in a Varian Medical Systems (Palo Alto, CA) delivery environment) plans due to the positive effects of delivering a more conformal dose to the treatment volume and sparing normal tissues and organs [1]. Because of the increasing complexity of IMRT and RapidArc plans used to treat different targets and due to the steep dose gradients, the delivered dose must be accurately measured [2]. This leads to one of the drawbacks for IMRT/RapidArc plan implementation: the time taken in order to assure that the patient dose distribution is met thoroughly and effectively before treatment through quality assurance (QA) [1].

One efficient QA measurement device is an electronic portal imaging device (EPID) [1]. Amorphous silicon (aSi) EPIDs have become more widespread for the use of dosimetry measurement and/or monitoring due to their attachment to the linear accelerator for time efficient measurement, real-time, digital feedback [1], allowing them to continuously read out the dose, and generating an integrated dose at the end of measurement [3]. Additionally, aSi EPIDs have a good spatial resolution (0.784 mm for the aS500 model or 0.39 mm for the aS1000), and the response of the aSi EPID is related to dose linearly [1, 2, 3].

However, the one drawback to aSi EPID imaging is non-uniform backscatter [3]. The initial radiation travels through materials uniform in the plane of acquisition, and upon exiting the imager, will travel through spatially variant material designs for EPID panel support. Some of the radiation is scattered back into the amorphous silicon portion of the panel and is detected as additional signal [3]. This results in differences being detected by the EPID that are dependent not only on position, but on field size as well [4].

In order to combat this problem, many have attempted to minimize the amount of backscatter, such as adding a thin layer of lead between the imager and the support arm [3]. This only minimizes the effects, but does not completely remove them, and the weight of lead backscatter shielding can cause sag in the mechanical arm positioning the EPID. Another option is to scale each individual pixel's response to a calibrated field based on irradiating the entire imager's surface [4]. However, this does not take into consideration the effects of the backscatter for different field sizes. Varian has created a Portal Dosimetry Pre-Configuration (PDPC) package, which utilizes a 2-dimensional pixel correction matrix to account for the asymmetric and off-axis response (due to penumbra and fluctuations in intensity) from the non-uniform backscatter [5]. However, this package applies the correction independent of varying field sizes and was created for maximum image agreement at a 15 x 15 cm^2 field, which may cause over or under correction of the backscattered radiation. The aim of this project is to correct the imager response as a function of field size for both off-axis and imaging arm backscatter variations; these corrections would be application-facing corrections, allowing them to be more robust than current corrections applied during absolute panel calibration.

2) Background

2.1) Quality Assurance and Verification

IMRT plans use a number of different field sizes with variable intensities in order to ensure the target volume (tumor) is precisely irradiated; each beam changes shape and intensity throughout the treatment [6]. RapidArc (or VMAT) is an advanced form of IMRT, with a continuously rotating gantry, whereas IMRT radiation is delivered as the gantry remains static [7]. Because of the precise nature of these treatments, it is extremely important to ensure that quality assurance goals are met; otherwise, the tumor may not be correctly treated, leading to parts of the tumor still intact or organs at risk receiving a higher dose than planned.

Because of the implications of QA being performed improperly, the verification for these plans must be done as efficiently and precisely as possible. The portal imager is an attractive solution to QA due to the fact that it is quick to setup, acquires data easily, and has a high pixel resolution [8]. However, in order to perform QA, the measured and expected dosimetric images must be obtained [8]. This poses an issue that the aSi panels in the EPID are not water-equivalent and display responses different from those observed in water [8].

Many solutions currently exist to convert the response of the imager to a portal dose. Some attempt to take the EPID's response image and change it to a dose in a certain depth of water, which is then compared to a dose in a water equivalent phantom that is calculated using the treatment planning system [8]. This approach is favorable because the patient dose is calculated with the same algorithm that calculates the portal dose image; however, the EPID image requires considerable processing to be converted from the response into dose in water [8].

Varian uses another approach in order to deal with the calculation of dosimetric images. Varian relies on the portal dose image prediction (PDIP) algorithm opposed to the patient dose

calculation algorithm to calculate the expected dose; this is calculated based on the treatment planning system photon intensity matrix, the total monitor units (MU) delivered, and the position of the field limiting collimation devices [8]. PDIP calculates the predicted dosimetric image via a single kernel convolution with the fluence matrix calculated from the treatment planning system (TPS) as shown in equation 1,

$$P = f' \otimes k * \left(\frac{SAD}{SDD}\right)^2 * OF(x,y) * PSF(x,y) \quad (1)$$

where, P is the predicted dosimetric image, f' is the deliverable TPS calculated fluence. SAD and SDD represent the source-to-axis distance and the source-to-detector distance of the machine and imaging panel, respectively. Output factors (OF) are measured as relative dose scaling factors specific to the aSi imaging panel, and phantom scatter factors (PSF) are calculated during the convolution calculation for field size correction factors. The results of this algorithm may not robustly describe the calculated image response for a plethora of machine geometries due to assumptions made during the EPID calibration process.

The dose calibration of the EPID consists of dark and flood fields, correcting for electronic noise and adjusting pixel gain to receive a flat dosimetric image at the open field across the detector; this is unacceptable for dosimetric purposes due to the beam's non-flatness, especially in the shoulder region [8]. Profile corrections can be used in order to achieve a more realistic response to the shape of the external beam [8]. In order to correct for the off-axis variation of the beam, the recommended solution is to use a profile for a 40 x 40 cm^2 field measured in a water phantom at either 5 cm or at the depth where the dose is a maximum (d_{max}), usually 1.5 cm for 6MV beams; the non-uniform backscattered radiation from the EPID's arm is not taken into account when using these profiles. This large image profile correction tends to over-estimate the out of field corrections for smaller field sizes taken on the EPID (maximum

field size 40 x 30 cm^2). Lastly, an absolute dose calibration step is required in order to create a correlation between measured pixel values and Portal Dosimetry's absolute measurement unit, calibrated units (CU).

Studies have shown the backscattered radiation can cause differences of a couple percent between the expected and measured doses, and although adding a thin layer of lead can minimize these differences, the added weight from the lead increases the weight of the EPID, which can cause uncertainties in the position of the EPID [4]. To correct the off-axis and asymmetric differences, the prediction model is often modified to account for the backscattered radiation [5]. The simplest and easiest way in a clinical setting is to use a 1-dimensional correction to fix the off-axis issues by adjusting the diagonal profile used [9]. However, this 1-dimensional profile cannot account for and fix the 2-dimensional asymmetric problems that arise from the backscatter, due to the fact that the PDIP algorithm assumes that the response will be symmetric about the beam's central axis [5].

To account for the off-axis and asymmetric discrepancies, a 2-dimensional profile has been introduced [10]. Varian's PDPC package uses a 2-dimensional correction to take the backscatter from the support arm into consideration [10]. However, the Varian PDPC package is optimized for a 15 x 15 cm^2 field size [5, 10]; because of this, the package can introduce errors for field sizes that are smaller or larger. In this study, by creating a 2-dimensional client-end correction that accounts for the backscatter as well as the field size, QA could be improved across all field sizes and geometries on average compared to the Varian PDPC package that is optimal at 15 x 15 cm^2 field sizes.

2.2) Dosimetric Leaf Gap

For IMRT and RapidArc treatment plans, in order to shape the beam to treat the desired target, a multileaf collimator (MLC) is used. The MLC is made up of specifically shaped bars of tungsten leaves, with rounded ends in order to maintain a constant penumbra at any off-axis position. Because the ends of these leaves are rounded, there exists some leakage radiation that will pass through the MLC [11, 12]. The dosimetric leaf gap (DLG) models the additional dose arising from the leaf tips in the treatment planning system [12]. This is important to take into careful consideration during QA due to the fact that a DLG that is unaccounted for can lead to an increase of dose to the patient, with studies showing that a MLC gap change of only 0.6 mm can lead to differences of 2% in the dose [12].

3) Methods and Materials

3.1) Materials

Two Varian TrueBeam linear accelerators were used on-site at the Varian Medical Systems facility in Las Vegas, NV, and Rhode Island Hospital in Providence, RI. All beams used were 6 MV photon beams. The EPID used was a Varian Portal Vision imaging panel model IDU20 EPID with aS1000 readout panel, which has an active area of 40 x 30 cm^2 made up of 1024 by 768 pixels. The phantom used for baseline measurements was a PTW (Freiburg, Germany) Octavius 4D. The water phantom used was a PTW MP3-M tank.

For data analysis and the creation of the correction profiles, MatLab R2014a (8.3.0.532) Student Version (Mathworks Inc., Natick, MA) was used.

3.2) Methods

3.2.1) Dosimetric Leaf Gap (DLG)

The DLG was measured by using Portal Dosimetry and an ion chamber. The output data was analyzed for the corrected transmission. This data from each of the techniques were measured from known MLC gaps (2 mm up to 30 mm) and normalized at a 10 mm gap. Each of the two data sets was extrapolated in order to find the x-intercept (corresponding to zero output), which is representative of the DLG. The average DLG, as well as DLG values above and below the measured values, were then used with plans in order to determine which DLG provided the best quality assurance agreement with the specified plan.

3.2.2) Beam Profiles

Four different beam profiles were used as the basis for the field size specific corrections created for comparison: 8 mm, 15 mm (d_{max}), and 50 mm water tank depth profiles at 40 x 40 cm^2, as well as the Varian PDPC package. First, the linac was calibrated according to TG-51

[13] protocol using the MP3-M scanning system and verified using solid water every day before measurements were taken. The water tank was set up in order to collect the diagonal profiles for 40 x 40 cm^2 fields, which were compared with the TrueBeam representative data for validation purposes. The positioning unit (PU), TrueBeam's imager arm, was calibrated to the absolute isocenter position using the isocenter calibration and isocenter verification modules on the TrueBeam. This creates a dynamic, gantry-angle specific correction for positioning unit sag. The DLG in Eclipse TPS (Varian Medical Systems, Inc., Palo Alto, CA) was changed to the experimental value obtained prior to these measurements to provide better results. The dosimetry mode of the imager was calibrated to each of the four profiles before shooting a set of verification plans (IMRT, Large Field IMRT, RapidArc) and fluence models for the MLC (qMLC). These were then analyzed, taking into account pass rates and gamma index, in order to understand the response of different profiles at different depths [14].

These measurements provide a valuable baseline for EPID calibration using known profile corrections. Lastly, the EPID is calibrated utilizing a 2-D unity matrix to nullify any existing off-axis response of the imaging panel. The previous plans are redelivered and exported in dose exchange format (DXF) and corrected programmatically for field size specific correction. After the package has been created, the same tests will be performed and compared with the initial calibrations to ensure that the package corrects for off-axis variations and backscatter better or comparable to the average across all field sizes.

3.2.3) Analysis of Plans

The pass rates (tolerances at 3% global dose difference, 3 mm distance to agreement) for the three diagonal fields and PDPC package plans were exported from Aria (Varian Medical Systems, Inc., Palo Alto, CA) and compared against their PDIP predicted images. The pass rates

for each field within a certain plan were analyzed and the average pass rate for a given plan using each different correction was calculated. These average pass rates were compared to one another to find out which of the four corrections models yields the best results, which we used as the baseline to compare to in this study.

3.3) Correction Profiles

DXF image files for 5 x 5 cm^2, 10 x 10 cm^2, 20 x 20 cm^2, and 30 x 30 cm^2 fields were delivered and exported without any correction profiles applied. These DXF files were corrected with the baseline profile that was determined by the previously mentioned comparison with standard portal dosimetry calibration methods. Because these corrections are normally optimized for one size (40 x 40 cm^2 diagonal field for the diagonal profiles and 15 x 15 cm^2 for the PDPC package), field size specific corrections should yield higher pass rates on average. These corrections were compared with uncorrected and PDPC flat fluences at each of the four field sizes. Then, pass rates of clinical plans (three RapidArc and two IMRT) with corrections of a 15 and 50 mm depth diagonal profile were analyzed with field-size specific 2-D corrections based on the previous method of correction (scanning tank profile specific measurements), as well as with an absolute EPID pixel correction profile (measured directly from pixel variation on the EPID). These pass rates will be analyzed at a 1% global, 1 mm threshold—more strict than clinical standards to ensure the best agreement possible. The pass rates were compared using the Wilcoxon signed-rank test with a p-value of < 0.05 indicating significance.

3.3.1) Open Field Diagonal Profiles

The 15 mm diagonal profile proved to be the best correction, so the correction profiles were modeled after this d_{max} diagonal profile. Open field water profiles were taken for the 15 mm diagonal profile at 5 x 5, 10 x 10, 20 x 20, and 30 x 30 cm^2 field sizes. These provided the

beam data for the profile at different x and y positions, as well as the dose at each location; because this is still a 1-dimensional diagonal profile, the x and y positions have the same values for each location. The radial distance (r) can thus be found by using equation 2,

$$r = \sqrt{x^2 + y^2} \tag{2}$$

This distance, along with the corresponding dose at that location, was imported into MatLab for each of the four field sizes.

Uncorrected DXF fluence files (5 x 5, 10 x 10, 20 x 20, and 30 x 30 cm^2 field sizes) were taken and imported into MatLab. A MatLab script was written to sweep through every pixel in these uncorrected fields, and if the pixel was within the field size, it would be provided a correction. The distance of the pixel from the center of the field was calculated, and the dose at this point was multiplied by the relative corrected dose; this was done by interpolating the dose at the location by using the imported diagonal profile beam data. By taking into account the radial distance away from the center, this field size specific correction takes into consideration the off-axis variations; additionally, because this is done and applied solely within the field, these corrections are more dynamic than a single 40 x 40 cm^2 diagonal beam profile applied to the entire imager.

3.3.2) Method 1: Equivalent Field Size d_{max} Profile Applied In-Field

Five patients' plans (three RapidArc and two IMRT) were applied a similar correction. Because these fields do not have square field sizes, the equivalent field size was determined using equation 3,

$$s = {}^{4A}/_{P} \tag{3}$$

where A is the area of the field, P is the perimeter, and s is the length of the equivalent square field sides. Because these fields do not have discreet fields corresponding with the four

measured profile field sizes, a weighted combination of the given profiles was used to create an equivalent profile. This was done by using the profiles for the larger and smaller fields than the equivalent field; by using equation 4, the relative weighing factors were found,

$$w_l = \frac{s_{equivalent}}{s_{large} - s_{small}} - 1 \quad (4)$$

where w_l represents the weighing factor of the large field, $s_{equivalent}$ is the length of the equivalent square field, s_{large} is the length of the larger square field correction profile, and s_{small} is the length of the smaller square field correction profile; the weighing factor for the smaller field is given by $1-w_l$.

When interpolating the dose for the new equivalent profile at the equivalent field size, the distance used is a ratio of the field sizes to give the dose at the relative position for the larger and smaller fields. For example, if the point being analyzed is at 60% of the max for an equivalent field, the doses to be weighed for the smaller and larger fields will be the doses at 60% instead of at the absolute position.

Because there is a rotation to the collimator applied, a matrix transformation was applied to find the new corners of the field; this was done for each corner of the field using equations 5 and 6,

$$x' = x\cos(\theta) + y\sin(\theta) \quad (5)$$

$$y' = y\cos(\theta) + x\sin(\theta) \quad (6)$$

where x' and y' are the new positions of the point, x and y are the non-rotated positions, and θ is the angle of rotation. Practically, because the location of the points is relative to the center of the imager, half of the total active area of the imager must be added to the x and y positions (512 and 384 pixels, respectively) after the rotations have occurred, since MatLab assumes the 0,0 point as the bottom left corner of the EPID. Once these new positions for the edges of the field had been

determined, another script was run using the *inpolygon* function to test whether each point is within the patient field; if it was within the field, the profile doses in the larger and smaller fields at the relative position was interpolated for, and this correction was applied to the new correction matrix.

3.3.3) Method 2: 40 x 40 cm^2 d_{max} Profile Applied In-Field

Similar to the previous method, this method applied only a dmax profile taken at the 40 x 40 cm^2 field size to the patient field. This used a similar script, with the only differences being that instead of using a weighted fit of two different profiles and the corrections at the relative positions, it simply used the 40 x 40 cm^2 d_{max} profile at the same distance.

3.3.4) Method 3: Equivalent Field d_{max} Profile Applied at Values Greater Than 50%

This correction relied on the equivalent field size and using weighing factors of square fields larger and smaller than the equivalent field, similar to method 1. However, instead of running through every point and checking if it was within the field, this method swept through every point, and if the value was greater than or equal to 50% of the maximum value in the uncorrected DXF file, the correction was applied. Because the dose should be minimal outside of the field, this correction is similar to method 1, and does not rely on a matrix transformation to establish the corners of the field.

3.3.5) Method 4: EPID Calibration Profile Applied at Values Greater Than 50%

Instead of using a water tank profile at d_{max}, this method relied on a profile which measured the differences between the measured and expected pixel values for the x and y axis of the EPID with no correction applied. By combining these two values, the difference in pixel response at a given location is obtained. A script ran through every pixel and applied the correction only if the response was greater than 50% of the maximum output, similar to method

3. These EPID measured field-size specific correction factors were measured utilizing the Eclipse Scripting Application Programming Interface (ESAPI) for Portal Dosimetry. Using ESAPI measured difference profiles between the predicted and acquired images were exported into a correction profile applied independently to the x-direction and y-direction.

3.3.6) Method 5: EPID Calibration Profile Applied In-Field

This correction method used the EPID pixel difference profiles and used the same code as methods 1 and 2 (matrix rotation and *inpolygon* function) to apply the correction only when it was inside of the field.

4) Results

4.1) Dosimetric Leaf Gap

The DLG data points from portal dosimetry and from the ion chamber (Table 1) were normalized and extrapolated to the x-axis (all done in MatLab), giving a DLG of 0.81 mm and 1.11 mm, respectively (Figure 1). The PTW Octavius 4D phantom was then used to test DLG values of 1.6, 1.1, 0.85, and 0.6 mm in order to see which DLG provided the best accuracy and agreement with the plan. An 8-field plan was calculated with varying DLG values in Eclipse TPS to test the different DLG values (at 2 mm, 2% pass rate criteria) (Table 2). The agreement in the measured values with the DLG closer to that of 0.81 mm indicates that the portal dosimetry DLG is more accurate and suitable for this TrueBeam machine, as well as the DLG being in the vicinity of 0.6 mm for the specific plan measured. The portal measured dosimetric leaf gap value is utilized during the dose calculations of our dynamic plans.

Table 1: Outputs for DLG Determination Using Ion Chamber and Portal Dosimetry

MLC gap (Millimeters)	2	5	8	10	12.5	15	20	25	30
Ion Chamber (Nano Coulombs)	1.40	2.14	2.87	3.36	3.97	4.58	5.79	7.02	8.24
Portal Dosimetry (Calibration Units)	6.86	10.97	15.09	17.84	21.28	24.71	31.60	38.47	45.36

Table 2: Different DLG Pass Rates

DLG (Millimeters)	0.6	0.85	1.1	1.6
Pass Rate	83.7%	83.5%	83.2%	80.9%

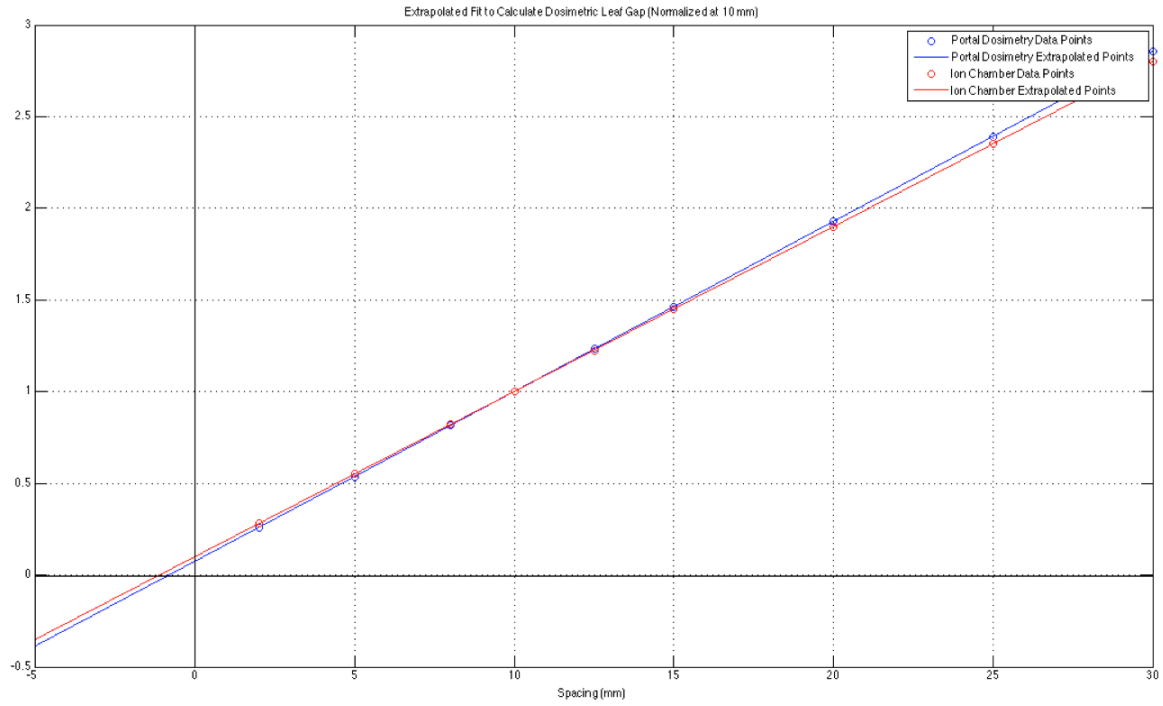

Figure 1: Graph of the Extrapolated DLG

4.2) Output Factors

Imager specific output factors for the three diagonal corrections as well as the PDPC package were acquired and compared in MatLab, with the average difference between all profiles and field sizes being 0.39%, with the maximum difference between any two output factors of the same field size being 0.73%. Due to this small difference, it was not necessary to measure output factors each time the calibration package is changed.

4.3) Pass Rate Comparisons

For each of the four corrections, the delivery of each plan (IMRT, LFIMRT, RA, and qMLC) was taken on the TrueBeam linac and all of the fields inside were analyzed with a distance to agreement (DTA) of 3.0 mm, and a global dose difference tolerance of 3.0%; the total percent of points which passed this threshold was analyzed, and a field is said to pass if 95.0% or

more of the points met this tolerance. The median pass rates of all the fields within a certain plan were compared for all four of the correction methods (Tables 3-6). The medians of all the plans as well as the plans and qMLC is shown in Table 7.

Table 3: Pass Rates for IMRT Plan Fields

IMRT Fields	8 mm	15 mm	50 mm	PDPC
AP_P1_0	99.1	99.7	98.9	98.8
AP_P1_1	96	99.4	95.9	97.6
LAO_P1_0	99	99.9	99	99.1
LAO_P1_1	98.4	98.8	98.6	98.7
LAO1_P1	97.6	99.8	97.2	97.1
LPO_P1_0	99.1	99.6	99.2	99.4
LPO_P1_1	94.5*	99.1	93.8*	94.4*
LPO1_P1_0	92.4*	98.5	92.6*	94.4*
LPO1_P1_1	98.7	99.1	98.7	98.5
RAO_P1_0	98.5	99.4	98.4	98.5
RAO_P1_1	99.1	99.8	99.4	99.4
RPO_P1_0	95.4	98.4	95.3	96.5
RPO_P1_1	99.3	99.5	99.4	99.5
Median (Range)	98.5 (92.4-99.3)	99.4 (98.4-99.9)	98.6 (92.6-99.4)	98.5 (94.4-99.5)

*denotes field did not pass criteria

Table 4: Pass Rates for LFIMRT Plan Fields

LFIMRT Fields	8 mm	15 mm	50 mm	PDPC
Field 1	96.4	99.4	94.5*	94.1*
Field 2	95.3	99.3	93.2*	91.1*
Field 3	97.7	98.1	95.8	95.7
Field 4	95.4	99.5	93.1*	92.1*
Field 5	95.3	98.8	93.4*	91.8*
Median (Range)	95.4 (95.3-97.7)	99.3 (98.1-99.5)	93.4 (93.1-95.8)	92.1 (91.1-95.7)

*denotes field did not pass criteria

Table 5: Pass Rates for RA Plan Fields

RA Fields	8 mm	15 mm	50 mm	PDPC
RA1	97.8	99.0	97.5	97.7
RA2	98.9	99.4	98.8	98.7
Median (Range)	98.35 (97.8-98.9)	99.2 (99.0-99.4)	98.15 (97.5-98.8)	98.2 (97.7-98.7)

Table 6: Pass Rates for qMLC Tests

qMLC Test	8 mm	15 mm	50 mm	PDPC
Aida	93.3*	97.2	95.5	98.1
DynChair	88.7*	96.4	87.6*	89.2*
FlatFluence	67.4*	80.7*	82.1*	87.1*
Median (Range)	88.7 (67.4-93.3)	96.4 (80.7-97.2)	87.6 (82.1-95.5)	89.2 (87.1-98.1)

*denotes field did not pass criteria

Table 7: Median Pass Rates

Plan Medians	8 mm	15 mm	50 mm	PDPC
IMRT	98.50	99.40	98.60	98.50
LFIMRT	95.4	99.3	93.4	92.1
RA	98.35	99.2	98.15	98.2
qMLC	88.70	96.40	87.60	89.20
Treatment Plan Median (Range)	97.75 (92.4-99.3)	99.40 (98.1-99.9)	97.35 (92.6-99.4)	97.65 (91.1-99.5)
Treatment Plan & qMLC Median (Range)	97.60 (67.4-99.3)	99.30 (80.7-99.9)	95.90 (82.1-99.4)	97.60 (87.1-99.5)

When examining all four plans, the 15 mm diagonal profile correction had the best agreement (p-value <0.002 when compared to the other three plans), and was thus used as the baseline. The pass rates of the 50 mm profile and the PDPC package were similar (p-value of

0.246), so we compared our corrections to the 50 mm profile as well, as it is the current correction used clinically.

4.4) Verification of Weighted Equivalent Profiles

Figure 2 shows the comparison between a calculated 15 x 15 cm^2 diagonal profile at d_{max} using the weighed 10 x 10 cm^2 and 20 x 20 cm^2 d_{max} profiles compared to the actual measured profile, suggesting an agreement.

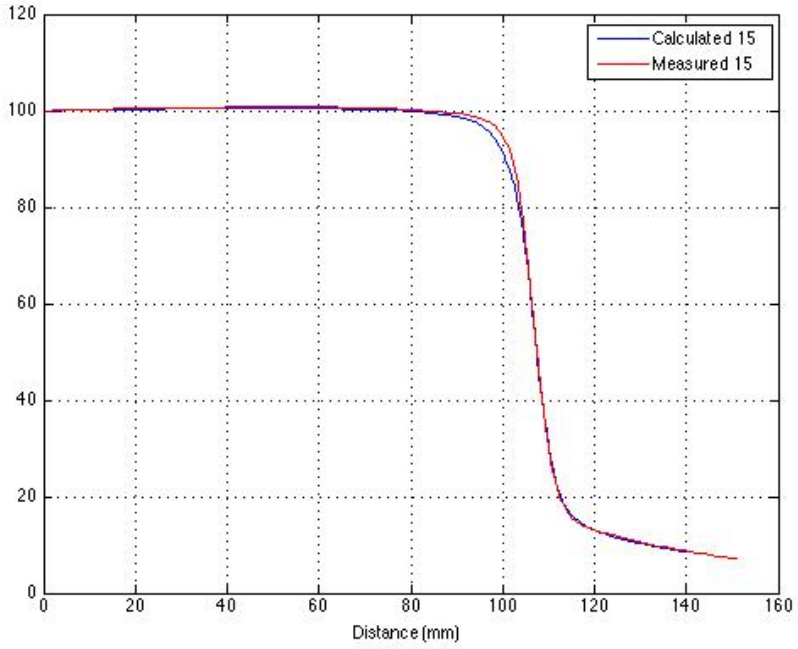

Figure 2: Measured 15 x 15 cm^2 d_{max} Profile Compared to Calculated Profile Using 10 x 10 cm^2 and 20 x 20 cm^2 d_{max} Profiles Using Weighing Factors.

4.5) Pass Rates for Correction Methods

The pass rates for all of the correction methods is shown in Table 8 along with the median pass rates and ranges for RapidArc, IMRT, and both combined.

Table 8: Pass Rates for Each Correction Method

Field	Uncorrected	D_{max}	50mm	Method 1	Method 2	Method 3	Method 4	Method 5
RA1_fld1	98.1	98.6	96.5	95.1	97.6	98.0	98.3	98.2
RA1_fld2	96.1	97.7	93.2	92.9	95.5	95.9	97.9	97.6
RA2_fld1	97.7	99.1	97.6	95.8	97.5	97.0	99.3	99.2
RA2_fld2	99.1	98.5	98.6	97.1	98.8	98.7	98.8	98.7
IMRT1_fld2	96.2	97.1	87.5	95.2	95.7	96.0	98.1	98.4
IMRT1_fld3	97.7	98.2	97.5	97.2	97.4	97.6	98.9	98.9
IMRT1_fld4	95.8	96.0	95.2	94.8	95.0	93.5	96.6	96.4
IMRT1_fld5	89.6	95.2	84.7	87.2	88.0	89.2	95.7	95.1
IMRT1_fld6	97.1	95.0	88.3	95.5	96.5	96.9	95.5	95.4
IMRT2_fld1	97.4	95.7	92.1	96.8	97.7	97.4	95.5	95.6
IMRT2_fld3	98.5	99.1	99.0	97.6	98.9	98.5	98.9	99.1
IMRT2_fld4	97.3	96.2	92.3	96.8	97.8	97.3	96.2	96.3
IMRT2_fld5	98.5	96.7	94.1	97.9	98.9	98.5	96.9	96.9
IMRT2_fld6	98.1	96.5	95.2	97.2	98.4	98.1	97.0	96.8
RA3_fld1	98.9	99.8	99.1	97.7	98.8	98.9	100	100
RA3_fld2	99.2	99.7	99.3	98.0	99.2	99.2	99.9	99.9
RA Median (Range)	98.5 (96.1-99.2)	98.85 (97.7-99.8)	98.1 (93.2-99.3)	96.45 (92.9-98.0)	98.2 (95.5-99.2)	98.35 (95.9-99.2)	99.05 (97.9-100)	98.95 (97.6-100)
IMRT Median (Range)	97.35 (89.6-98.5)	96.35 (95.0-99.1)	93.2 (84.7-99.0)	96.8 (87.2-98.0)	97.55 (88.0-98.9)	97.35 (89.2-98.5)	96.75 (95.5-98.9)	96.6 (95.1-99.1)
All Median (Range)	97.70 (89.6-99.2)	97.4 (95.0-99.8)	95.2 (84.7-99.3)	96.8 (87.2-98.0)	97.65 (88.0-99.2)	97.5 (89.2-99.2)	98.0 (95.5-100)	97.9 (95.1-100)

Wilcoxon signed-rank tests were performed, with the p-values compared to both common clinical correction methods with a 5% significance level. If a p-value is less than 0.05, it can be viewed that there is strong evidence to reject the null hypothesis—in our case, that the field size specific corrections will not beneficially affect the QA analysis. These p-values for the correction methods tested against the standard 50 mm and d_{max} profile corrections is shown in Table 9 (this is not performed for method 1, since it had the lowest pass rates of all of them).

Table 9: Wilcoxon Signed-Rank Test P-Values for Correction Methods 2-5

P-values	Method 2	Method 3	Method 4	Method 5
p-value (50 mm)	0.0193*	0.0271*	0.0006*	0.0005*
p-value (d_{max})	0.7263	0.4179	0.0139*	0.0278*

*$p < 0.05$

These results indicate that methods 4 and 5 provided the best corrections compared to the common clinical correction 50 mm and d_{max} 1-dimensional 40 x 40 cm^2 field size diagonal profiles, with method 4 proving to be better than the d_{max} profile at a smaller significance level. The 20 x 20 cm^2 open fields for the uncorrected, 50 mm, dmax, and method 4 corrected profiles are shown in Figures 3-4, 6, and 8. The uncorrected open field (Figure 3) shows failure rates radially from the center around the entire field because off-axis variances and backscatter are not accounted for. The 50 mm 40 x 40 cm^2 field diagonal profile correction applied (Figure 4) fails radially due to the overcorrection of off-axis variations. Figure 5 shows the x-axis profile, demonstrating the off-axis differences due to the lack of backscatter component in the horizontal direction. The d_{max} 40 x 40 cm2 field diagonal profile correction applied (Figure 6) accounts for the off-axis variations very well, however, does not account for the asymmetric backscatter from the imager arm. Figure 7 shows the y-axis profile, showing the backscatter component in the bottom of the profile. The method 4 correction applied (Figure 8) accounts for not only the off-axis variations (Figure 9), but also the backscatter component (Figure 10).

A comparison of method 4 and 40 x 40 cm^2 dmax profile pass rate comparisons for two fields are shown in Figures 11-12 (both figures will have a standard 40 x 40 cm^2 d_{max} profile on the left, with method 4's correction on the right).

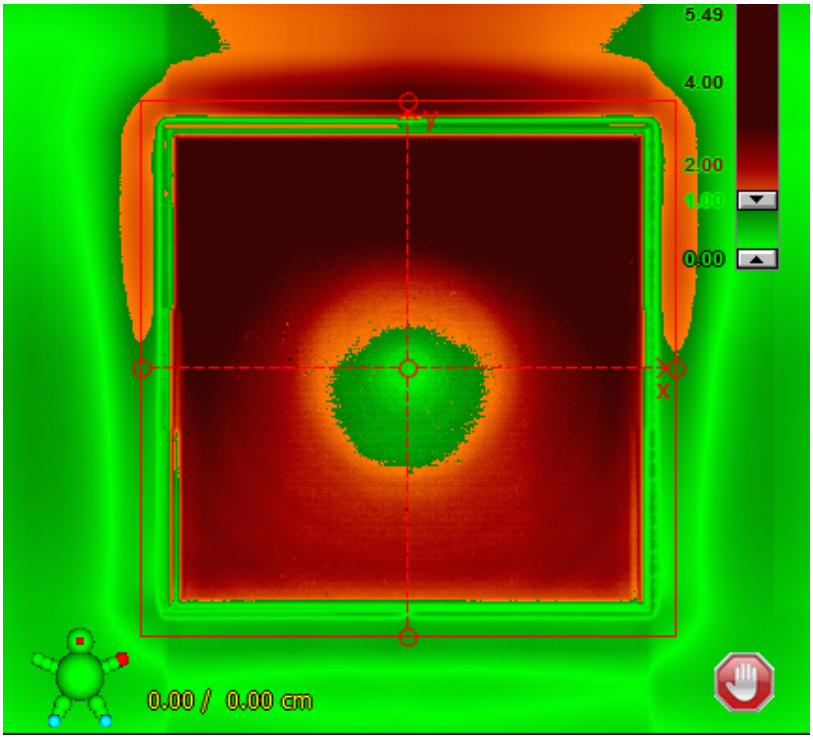

Figure 3: 20 x 20 cm^2 Open Field with No Correction

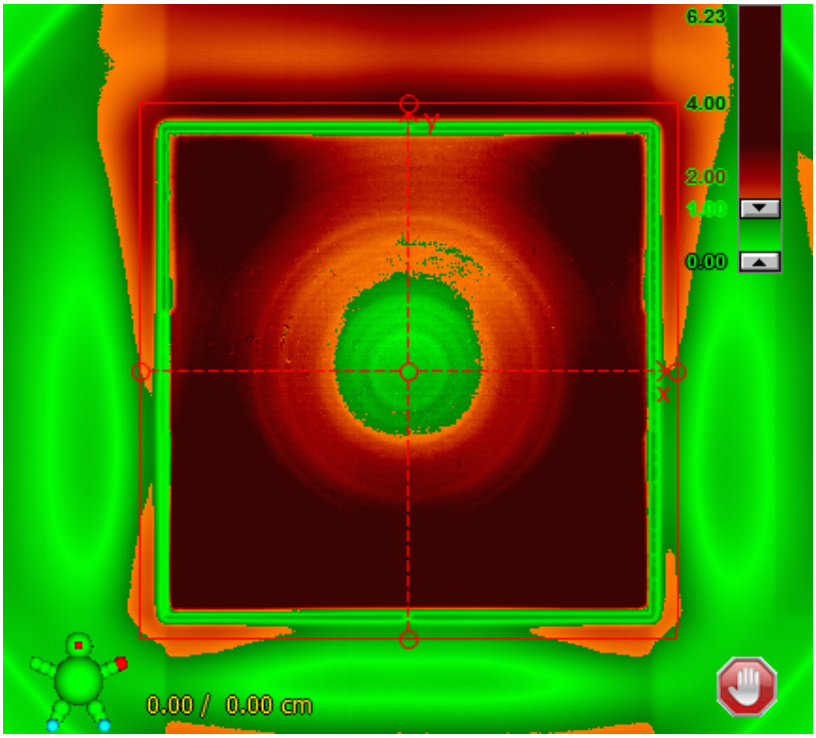

Figure 4: 20 x 20 cm^2 Open Field with 50 mm 40 x 40 cm^2 Field Diagonal Profile Correction

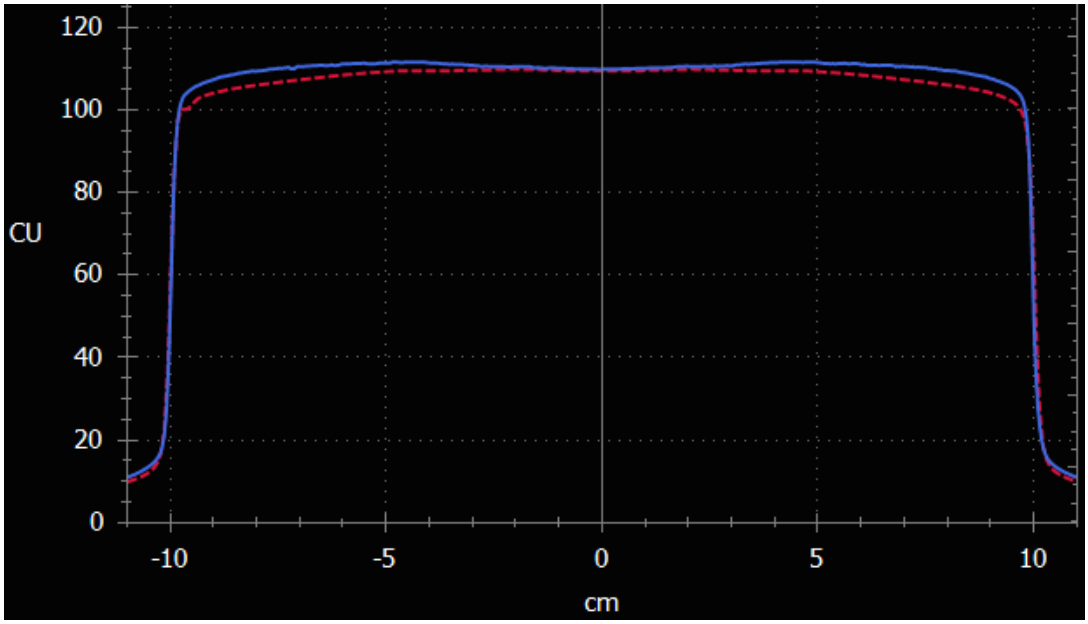

Figure 5: Off-Axis Variations Being Overcorrected for in Measured 50 mm Profile Correction (Solid Line) vs. Predicted (Dashed Line)

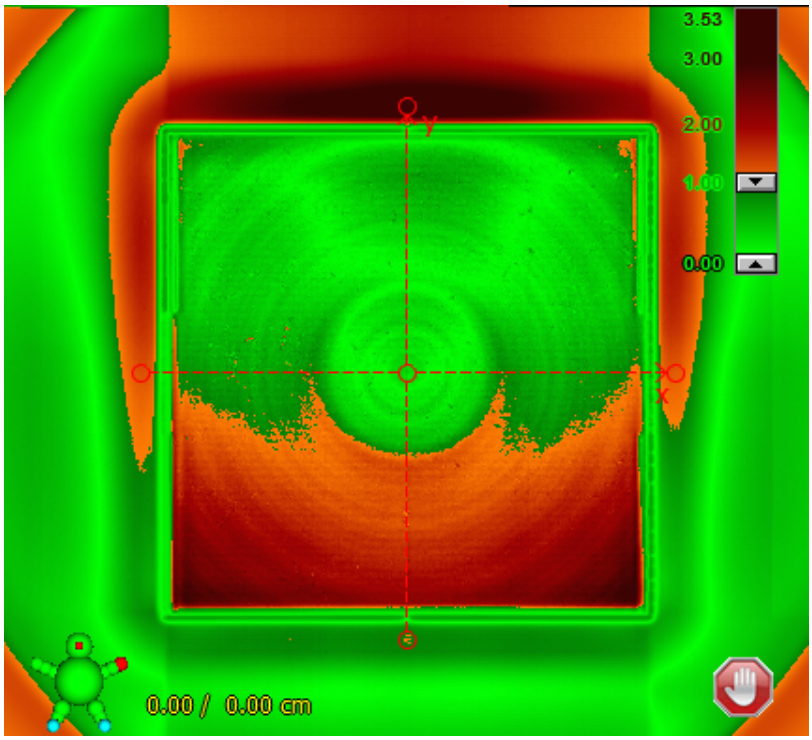

Figure 6: 20 x 20 cm^2 Open Field with d_{max} 40 x 40 cm^2 Field Diagonal Profile Correction

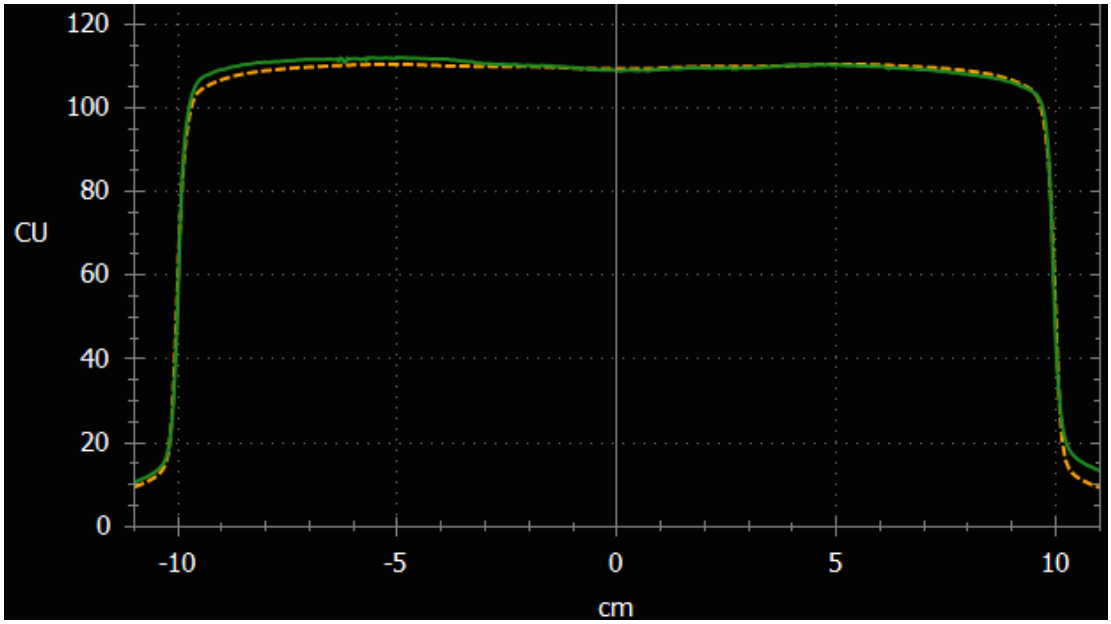

Figure 7: Asymmetric Backscatter Component in Measured d_{max} Profile Correction (Solid Line) vs. Predicted (Dashed Line)

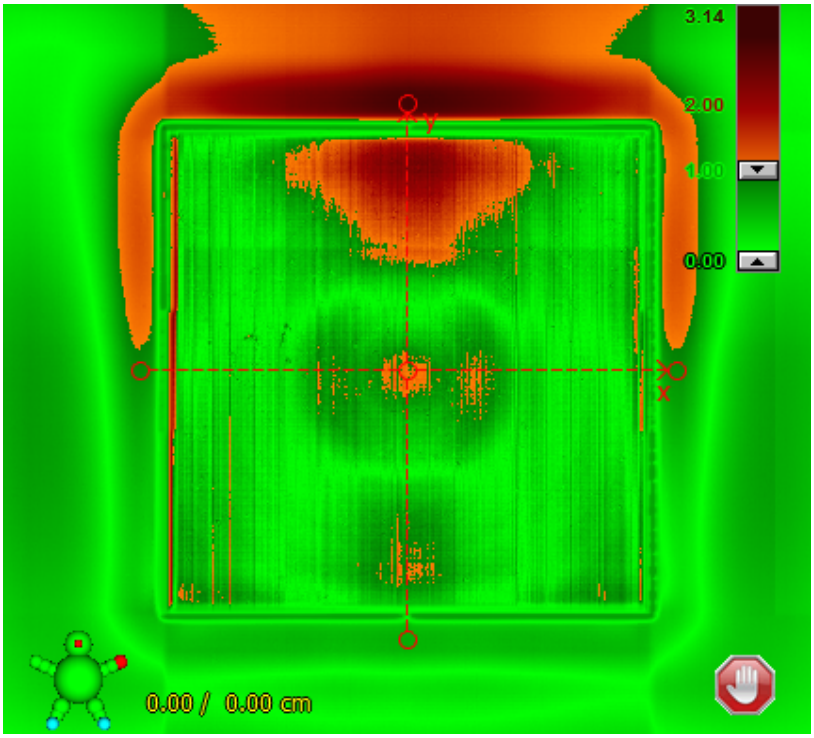

Figure 8: 20 x 20 cm2 Open Field with Method 4 Correction

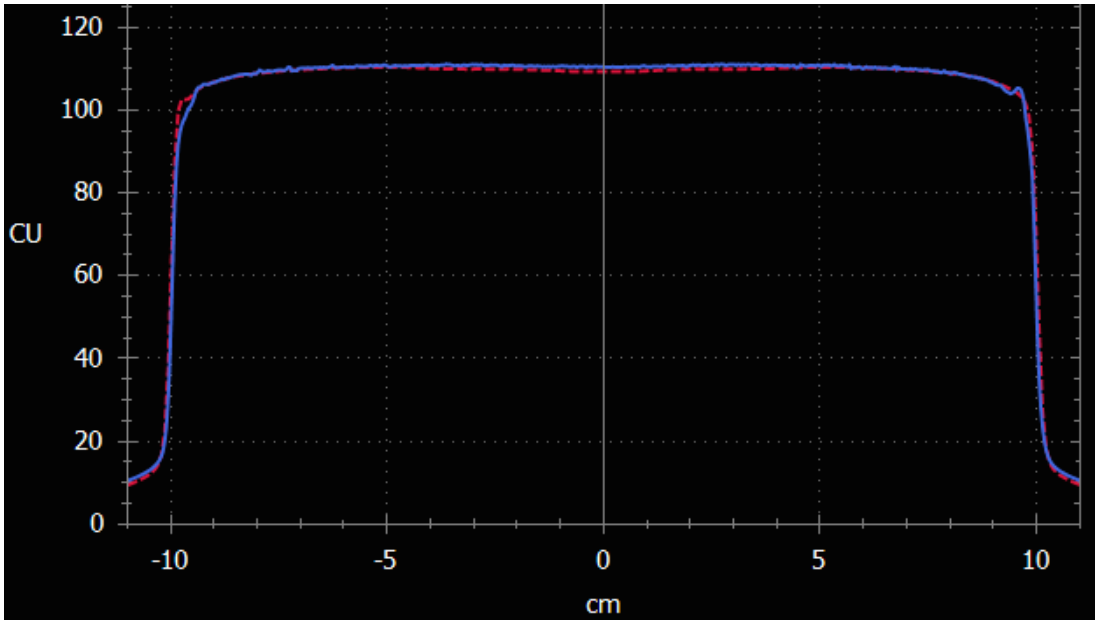

Figure 9: Agreement in Off-Axis Variations in Method 4 Measured Profile (Solid Line) vs. Predicted (Dashed Line)

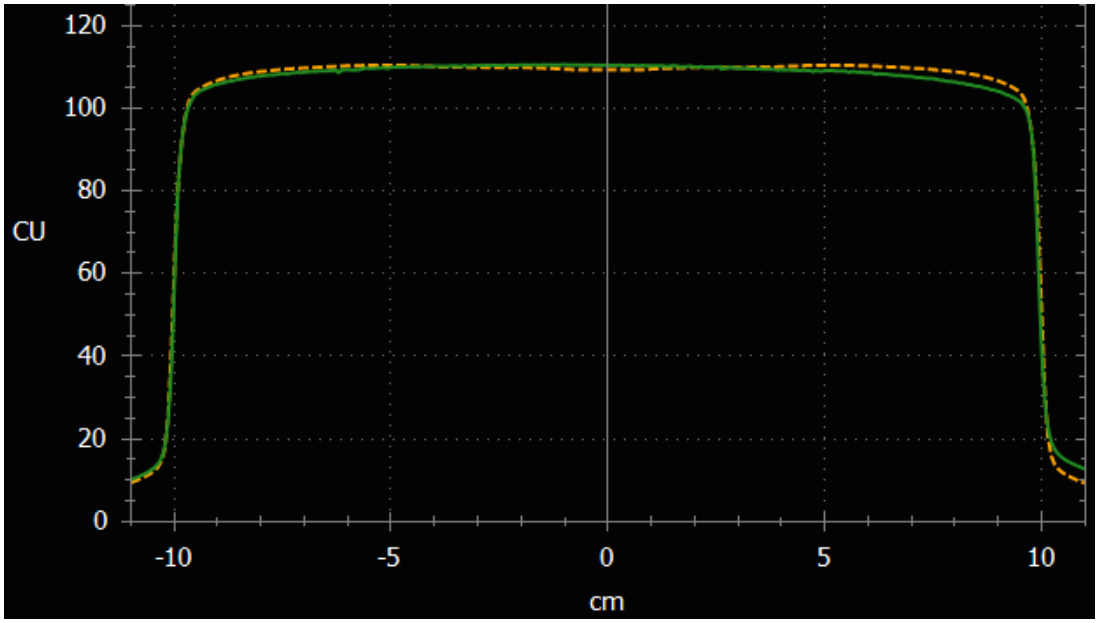

Figure 10: Backscattered Component Accounted for in Method 4 Measured Profile (Solid Line) vs. Predicted (Dashed Line)

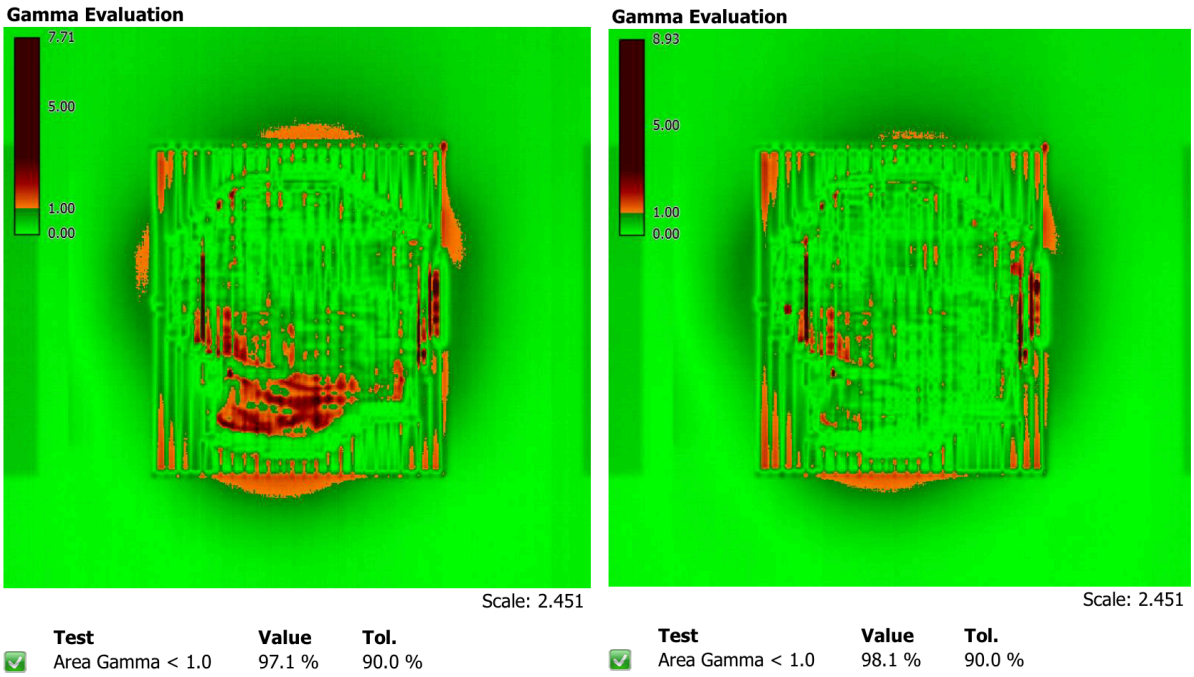

Figure 11: IMRT1_fld2 Gamma Pass Rate Comparisons

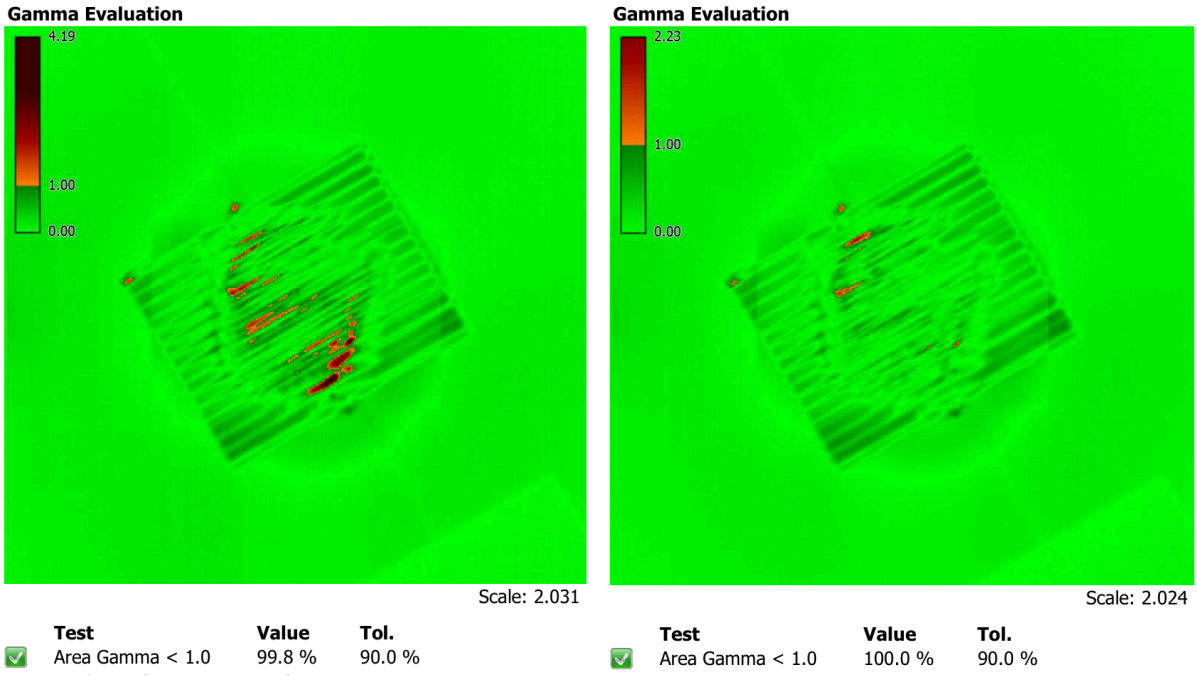

Figure 12: RA3_fld1 Gamma Pass Rate Comparisons

5) Discussion

Although it is not surprising that the d_{max} profile was better than the 50 mm profile, the worse agreement of the PDPC package to the plans was surprising. Additionally, the performance of the PDPC package and the 50 mm profile were very similar in comparing the results of IMRT, LFIMRT, and RA. This seems as if the 1-dimensional 50mm profile can perform similarly to the 2-dimensional PDPC package. This was not examined closely in this study, but would be a future direction of our work.

When applying correction method 1, the passing rates were not greatly improved, motivating us to investigate different methods. The fact that method 1's correction was worse than both 50 mm and d_{max} 40 x 40 cm^2 field profiles led to using a 40 x 40 cm^2 field d_{max} profile and only applying it inside the field and at values above 50% of the maximum. This led to some promising results, although not as good as the 40 x 40 cm^2 d_{max} profile, it yielded better results than the 50 mm profile. The last two correction methods involved taking a pixel correction profile, which uses the response of the EPID. This more accurately measures the response compared to a water profile, since a water profile assumes radial symmetry. The water profile would work in the x-direction since it accounts for the horns, but would not account for the asymmetric backscatter in the y-direction. However, the pixel correction profile takes this effect into account. This could achieve better results in theory if a pixel correction for every pixel was calculated instead of simply sweeping across the center of the EPID in the x and y direction, as it would account for more fluctuations due to the horns in the x-direction and the asymmetries in the y-direction.

6) Conclusion

In this study, we demonstrated that the best current correction method for factoring in off-axis and asymmetric backscatter when using portal dosimetry for QA is by using a 40 x 40 cm^2 d_{max} diagonal water profile. Although other correction techniques exist (50 mm profiles or the PDPC correction package), on average, pass rates using the d_{max} profile for the clinical QA fields tested reported closer matches. Even though this 1-directional method assumes a radial-equivalent response in the EPID and corrects the off-axis effects, it still does not properly address the asymmetric backscatter from the imager arm. In order to combat this problem, Varian's PDPC package uses a 2-dimensional correction, but due to the fact that it is only optimized for a 15 x 15 cm^2 field, it has a similar level of agreement as the 50 mm 1-dimensional profile. By taking into consideration the field size, or by understanding that the edge of the field size will have around a 50% response of the maximum, the backscatter component can be fixed more accurately. Additionally, instead of using a water profile, using the response from the uncorrected EPID pixels to create a difference profile in both the x and y direction, the off-axis and asymmetric components can be compensated for.

Using Method 4's correction, the asymmetric backscatter will be accounted for as a function of position on the imager instead of using the radial distance, which does not account for it accurately. This correction would be applied whenever IMRT QA is performed, allowing it to be more dynamic than a single correction applied during absolute panel calibration. When this 2-dimensional method is used for EPID correction, it gives statistically better (approximately 98.6% of the time) pass rates for IMRT QA when compared to the common clinical correction methods (50 mm and d_{max} 40 x 40 cm^2 field water profiles) as well as Varian's 2-dimensional PDPC package which attempts to correct for backscatter.

7) References

1. Van Esch, A., Depuydt, T., & Huyskens, D. P. (2004). The use of an aSi-based EPID for routine absolute dosimetric pre-treatment verification of dynamic IMRT fields. *Radiotherapy and Oncology*, *71*(2), 223-234.

2. Rowshanfarzad, P., Sabet, M., O'Connor, D. J., & Greer, P. B. (2012). Impact of backscattered radiation from the bunker structure on EPID dosimetry. *Journal of Applied Clinical Medical Physics*, *13*(6).

3. Ko, L., Kim, J. O., & Siebers, J. V. (2004). Investigation of the optimal backscatter for an aSi electronic portal imaging device. *Physics in Medicine and Biology*, *49*(9), 1723.

4. Berry, S. L., Polvorosa, C. S., & Wuu, C. S. (2010). A field size specific backscatter correction algorithm for accurate EPID dosimetry. *Medical Physics*, *37*(6), 2425-2434.

5. Hobson, M. A., & Davis, S. D. (2015). Comparison between an in-house 1D profile correction method and a 2D correction provided in Varian's PDPC Package for improving the accuracy of portal dosimetry images. *Journal of Applied Clinical Medical Physics*, *16*(2).

6. IMRT (Intensity Modulated Radiation Therapy). Retrieved October 23, 2015, from https://www.varian.com/oncology/treatment-techniques/external-beam-radiation/imrt

7. VMAT (Volumetric Arc Therapy). Retrieved October 23, 2015, from https://www.varian.com/oncology/treatment-techniques/external-beam-radiation/vmat

8. Van Esch, A., Huyskens, D. P., Hirschi, L., & Baltes, C. (2013). Optimized Varian aSi portal dosimetry: development of datasets for collective use. *Journal of Applied Clinical Medical Physics*, *14*(6).

9. Bailey, D. W., Kumaraswamy, L., & Podgorsak, M. B. (2009). An effective correction

algorithm for off-axis portal dosimetry errors. *Medical Physics*, *36*(9), 4089-4094.

10. Varian Medical Systems. (2012). *Installation and Verification of the Portal Dosimetry Pre-Configuration Package 1.0*. [Bulletin].
11. Kielar, K. N., Mok, E., Hsu, A., Wang, L., & Luxton, G. (2012). Verification of dosimetric accuracy on the TrueBeam STx: Rounded leaf effect of the high definition MLC. *Medical Physics*, *39*(10), 6360-6371.
12. Mei, X., Nygren, I., & Villarreal-Barajas, J. E. (2011). On the use of the MLC dosimetric leaf gap as a quality control tool for accurate dynamic IMRT delivery. *Medical Physics*, *38*(4), 2246-2255.
13. Almond, P. R., Biggs, P. J., Coursey, B. M., Hanson, W. F., Huq, M. S., Nath, R., & Rogers, D. W. O. (1999). AAPM's TG-51 protocol for clinical reference dosimetry of high-energy photon and electron beams. *Medical physics*, *26*(9), 1847-1870.
14. Low, D. A., Harms, W. B., Mutic, S., & Purdy, J. A. (1998). A technique for the quantitative evaluation of dose distributions. *Medical physics*, *25*(5), 656-661.

8) Curriculum Vitae

Remy Manigold
9450 Showplace Dr.
La Mesa, CA 91941
remymanigold@gmail.com
(619) 867-1313

Education

8/2014 – 5/2016 **University of Nevada Las Vegas**
-M.S. in Medical Physics
-Working on thesis with Varian Medical Systems under Matthew Schmidt
-Thesis: "Creating a Dynamic, Multi-Purpose Correction for Multiple Geometries and Field Sizes to Account for Off-Axis and Asymmetric Backscatter with Varian Portal Dosimetry"

9/2010 – 6/2014 **California Polytechnic State University, San Luis Obispo**
-B.S. in Physics

Work and Research Experience

8/2015 – 12/2015 **University of Nevada Las Vegas, NV**
Graduate Assistant for Dr. Bing Ma (Principles of Computed Tomography)

Summer 2015 **University of California San Diego, CA**
Volunteer work with Dr. Laura Cervino working on a GUI to track fiducials for motion management

Spring 2014 **California Polytechnic State University, San Luis Obispo, CA**
Modern Physics Grader, Dr. Katharina Gillen

Spring 2013 **California Polytechnic State University, San Luis Obispo, CA**
Modern Physics Grader, Dr. Thomas Gutierrez

Summer 2012 **University of Pittsburgh Medical Center Horizon, Shenango Valley, PA**
Shadowed Medical Physicist, Dr. Tony Combine

Honors and Awards

8/2015 – Present **Graduate Assistantship (merit-based)**
University of Nevada Las Vegas

Memberships, Activities, & Skills

Society Member

8/2015 – Present **Vice President**
UNLV Health Physics Society Student Chapter

Other Activities

11/07/2015	**Boy and Girl Scout Nuclear Science Badge, Las Vegas, NV** Volunteered to teach scouts about nuclear science in order to get their badge.
3/2011 – 9/2011	**W.O.W, California Polytechnic State University, San Luis Obispo, CA** Week of Welcome Orientation training to become a leader to introduce new students to the campus and town, as well as important issues relevant to being a college student
Summer 2009	**Alvarado Hospital Medical Center, San Diego, CA** Sterile Processing Volunteer, helped set up carts for surgeries.
Spring 2007/2009	**Tennis Special Olympics, San Diego, CA** Volunteer in order to help run the Tennis Special Olympics held in San Diego

Languages

Fluent in English and French

Additional Skills

- MatLab experience (Digital Acquisition, Data Analysis, Graphical User Interfaces, etc.)
- Experience with TrueBeam Service Mode and TG-51